Block Copolymer Domain Reorientation in an Electric Field: An in-Situ Small-Angle X-ray Scattering Study

J. DeRouchey, T. Thurn-Albrecht, and T. P. Russell*

Polymer Science and Engineering Department, University of Massachusetts−Amherst, Amherst, Massachusetts 01003

R. Kolb

ExxonMobil Research and Engineering Company, Annandale, New Jersey 08822

Received June 2, 2003; Revised Manuscript Received January 28, 2004

ABSTRACT: Using in-situ small-angle X-ray scattering, the electric field induced orientation of symmetric block copolymers of polystyrene and polyisoprene was investigated. Alignment of the lamellar microdomains parallel to the electric field was achieved within minutes to a high degree of orientation. Analysis of the scattering patterns indicated that, during alignment of the lamellar microdomains, the material goes through an intermediate state with substantially reduced long-range order. After orientation, the sample consists of many small grains with the lamellae being oriented parallel to the electric field and a random orientation in the plane perpendicular to the field.

Introduction

Self-assembling systems that can order into periodic arrays of nanoscopic structures have potential use in applications ranging from optics to microelectronics. A prominent example of such systems are block copolymers exhibiting a microphase structure on a mesoscopic length scale while offering tunability of size and structure by chemistry in addition to relatively simple processing.[1−3] Achieving uniform orientation in these materials, however, is not trivial. While shearing[2] provides an effective route to orient the copolymer microdomains in the bulk, it is not applicable to thin films. Previously, electric fields,[4−9] controlled interfacial interactions,[10,11] and solvent evaporation[12,13] have been used to orient such samples, resulting in highly oriented and ordered block copolymer films. These films provide a unique platform as templates to fabricate functional nanostructured materials.[14−19]

Microphase-separated block copolymers contain grains of ordered microdomains where the grains, on average, have no preferred spatial orientation. In the presence of an electric field, this symmetry is broken, and the microdomains orient such that the interfaces between the microdomains align parallel to the electric field lines.[4−7] Little is known, however, regarding the mechanism by which the orientation of the microdomains proceeds or the influence of the field on the microdomain structure during alignment. Previously, Amundson et al. have inferred a mechanism of defect movement based on the characterization of the structure in bulk after annealing under a field.[5,6] More recently, Krausch and co-workers[20,21] have suggested both defect translation and grain rotation as possible mechanisms in studies on block copolymer solutions. Additionally, simulations were used to provide some insight[22,23] and gave indications supporting both of these mechanisms.[24] It was suggested that a breakup of microdomains by small scale undulations typically occurs close to the order−disorder transition, while grain rotation happens in more strongly phase-separated systems.[24] Previously, we have shown for a block copolymer melt with cylindrical microdomains that an electric field can not only induce a reorientation of microdomains in an ordered but misaligned sample but also direct growth of microdomains during formation at the ordering transition.[25]

Here we present an in-situ synchrotron small-angle X-ray scattering (SAXS) study on the alignment of an ordered lamellar block copolymer melt in an electric field, including a more detailed analysis of the scattering patterns in the intermediate and final state of alignment. Results indicate that orientation proceeds via a disruption or disordering of the original morphology, leading to a transient change in periodicity and a substantial loss of long-range order. The final state consists of many small grains which appear to have undergone alignment independently.

Electric Field Effects

When a body with a dielectric constant ϵ is placed in an electric field $\vec{E}_0$, the difference in polarization between the body and the surroundings will induce charges on the surface of the body. These surface charges give rise to a depolarization field $\vec{E}_p$ superposed on the external field, $\vec{E}_0$. For an anisotropic body, the surface charges and, therefore, $\vec{E}_p$ will depend on its orientation. The free energy can be written as[26]

$$F = F_0 + F_{el} = F_0 - \frac{1}{2}\int_V \vec{E}_0 \cdot \vec{P}\, dV \qquad (1)$$

where F_{el} is the orientation-dependent electrical contribution to the free energy, and F_0 contains all the contributions to the free energy independent of the applied field. $\vec{P}$ is the polarization of the dielectric body having a volume V. The polarization is proportional to the total electric field $\vec{E}_0 + \vec{E}_p$,

$$\vec{P} = \epsilon_0 \chi \vec{E} = \epsilon_0 \chi (\vec{E}_0 + \vec{E}_P) \qquad (2)$$

where χ is the polarizability which for an isotropic material is a constant. Evaluation of eq 1 requires solving Maxwell equations subject to the boundary conditions for the electric field at the interface.[26] For

10.1021/ma034739f CCC: $27.50
Published on Web 03/12/2004

Table 1. Characteristics of Copolymers

	$M_{n,PS}$ (kg/mol)	PDI_{PS}	$M_{n,copolymer}$ (kg/mol)	$PDI_{,copolymer}$	T_{ODT} (°C)
57K PS−PI	32.05	1.02	57.3	1.021	307[a]
43K SIS	9.8	1.031	43.1	1.022	∼165[b]

[a] T_{ODT} calculated. [b] Experimentally observed.

the case of a single lamella having a large lateral extension, the free energy, F, is given by

$$F = F_0 - \frac{1}{2}E_0^2\epsilon_0(\epsilon - 1)\left(\cos^2\beta + \frac{\sin^2\beta}{\epsilon}\right)V \quad (3)$$

where ϵ_0 is the permittivity in a vacuum, V is the volume of the lamellae, and β is the angle between the electric field $\vec{E}_0$ and the lamellar surface. F is minimized when $\beta = 0$, i.e., when the electric field is parallel to the lamellar surface. The difference in the free energy between lamellar orientation parallel and perpendicular to the electric field is given by

$$\Delta F = F_{||} - F_{\perp} = -\frac{1}{2}E_0^2\epsilon_0\frac{(\epsilon - 1)^2}{\epsilon}V \quad (4)$$

and the torque acting to rotate lamellae inclined at an angle β to the electric field is given by

$$\vec{K} = \vec{P} \times \vec{E}_0, \quad |\vec{K}| = E_0^2\epsilon_0\frac{(\epsilon - 1)^2}{\epsilon}V\cos\beta\sin\beta \quad (5)$$

If the surrounding medium has a dielectric constant ϵ_{ext}, ϵ has to be replaced by ϵ/ϵ_{ext} and ϵ_0 by $\epsilon_0\,\epsilon_{ext}$, leading to

$$|\vec{K}| = E_0^2\epsilon_0\frac{(\epsilon - \epsilon_e)^2}{\epsilon}V\cos\beta\sin\beta \quad (6)$$

Implicitly assumed in these calculations is that the boundaries between the lamellar microdomains are sharp, which is justified in the strong segregation regime. Calculations for the weak segregation regime were previously published.[5,6] By restricting the above considerations to single lamellae, we also neglect interactions between dipoles induced in neighboring lamellae.

Experimental Section

Materials. A symmetric diblock copolymer of polystyrene and polyisoprene, PS-*b*-PI, having a weight-average molecular weight of 5.7×10^4 and a polydispersity index (PDI) of 1.02 was synthesized anionically, at room temperature, in benzene using *sec*-butyllithium as the initiator. The molecular weights of both blocks were determined by size exclusion chromatography (SEC), calibrated against PS standards, with a UV detector. Since the reaction was performed in a nonpolar solvent with a Li initiator, the isoprene blocks will have a high 1,4 component (∼93%) with a minor 3,4 addition component (∼7%).[27] A PS-*b*-PI-*b*-PS triblock copolymer, denoted SIS, was similarly prepared via the sequential additions of styrene, isoprene, and styrene to yield volume fractions of 0.25, 0.5, and 0.25, respectively. SEC data corresponding to the first styrene block and the final copolymers are given in Table 1.

The order−disorder transition (ODT) temperature for the PS-*b*-PI block copolymer can be calculated[28] by

$$(\chi N)_{ODT} = 10.5 + 41\boldsymbol{N}^{1/3} \quad (7)$$

where χ is the Flory−Huggins interaction parameter and $\boldsymbol{N} = (b^6/V^2)N$. Here, b is the segment length with volume V and N is the total number of monomers in the copolymer. The temperature dependence of χ is given by[29,30]

$$\chi(T) = \frac{66}{T} - 0.0937 \quad (8)$$

The estimated ODT temperature for the 57K PS-*b*-PI diblock copolymer is 307 °C. Experiments were performed at ∼170 °C, which is above the glass transition temperatures of both blocks but well below the order-to-disorder and degradation temperatures.[31] The SIS was experimentally found to have a T_{ODT} of ∼165 °C. The in situ alignment of the triblock material was, therefore, performed at 130 °C, i.e., above the T_g of the copolymer but below the ODT.

Sample Preparation. Copolymer films were prepared using a Stanat 10 in. × 13 in. two-roll calendar to obtain films of uniform thickness in the range 80−120 μm. These films were placed between two electrodes consisting of 12.7 μm Kapton sheets, onto which 100 nm of Al was evaporated on one side. To avoid electrical shorts, one electrode was placed in direct contact with the copolymer while the other electrode was placed with the Kapton side facing the polymer. All samples were preannealed for 4 h at 120 °C under vacuum to ensure good contact and minimize air gaps between the polymer and the electrodes. The samples were heated to 170 °C, and an electric field was applied. Exposure of the sample to elevated temperatures was limited to a few hours to minimize degradation and/or cross-linking of the copolymer.

X-ray Scattering. Time-resolved small-angle X-ray scattering experiments (SAXS) were performed at the National Synchrotron Light Source (NSLS) on beamline X10A. 8 keV X-rays from a double-bounce Ge monochromator ($\Delta E/E = 4 \times 10^{-4}$) were used with a spot size of 1.0 mm (horizontal) by 0.7 mm (vertical) at the sample. A Bruker Smart 1500 CCD 2-D detector, located ∼2.2 m from the sample, was used to record the scattering pattern. The flight path between the sample and detector was filled with He to eliminate air scattering, and a silver behenate standard was used for angular calibration. Typical exposure times for a 100 μm sample were 2 s. Samples were mounted in a heated sample chamber consisting of two metal plates with a 2 mm × 15 mm horizontal slit. The heating chamber was placed on a goniometer, such that α, the incidence angle of the beam on the sample defined relative to the surface normal, could be varied from 0° (normal to the surface) to 60°.

Dielectric Measurements. Measurements of the dielectric constant at high temperature were made with a Novocontrol BDC-S system. Measurements were made at low frequency (10 Hz) and at a constant temperature of 170 °C. The samples were kept between gold-plated stainless steel plates of 20 mm diameter. Samples were gold plated to about 30 nm thickness on both sides prior to measurements.

Results

The scattering from a lamellar microphase-separated block copolymer exhibits a maximum at a scattering vector q_{max}, corresponding to the period, L, of the lamellar microdomains ($q = 2\pi/L$). The scattering vector q is defined as $q = 4\pi/\lambda\sin\theta$, where λ is the wavelength and 2θ is the scattering angle. The orientation of the copolymer microdomains can be determined from the azimuthal dependence of scattering. We define γ as the angle between the surface normal and the lamellar normal. For lamellae oriented parallel to the substrate surface, i.e., with the lamellar normal parallel to the substrate normal ($\gamma = 0°$), as illustrated in Figure 1A, scattering is only seen when the incidence angle $\alpha = 90°$. In this case, the incident beam would be in the plane of the film. In the opposite extreme, when the lamellae are oriented normal to the surface ($\gamma = 90°$), with a random in-plane orientation of the grains, two meridional spots are observed for all $\alpha > 0°$, as illustrated in Figure 1B. For $\alpha = 0°$, an isotropic ring

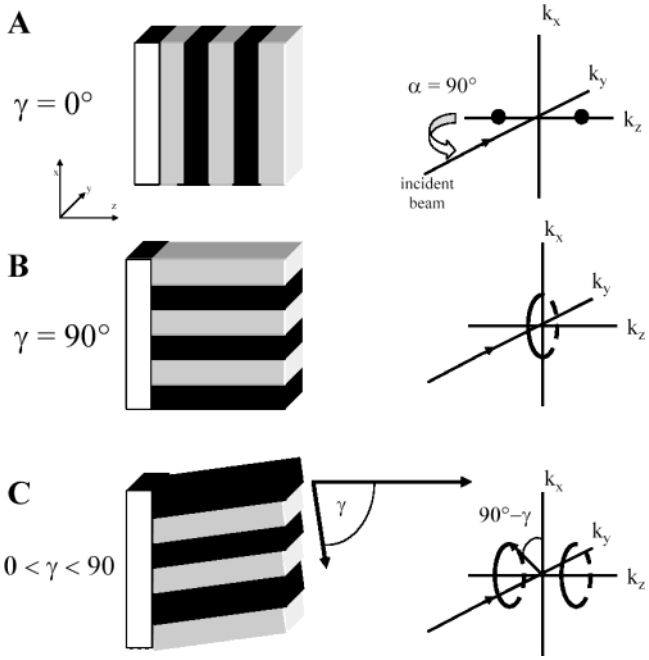

Figure 1. Schematic drawing of oriented lamellae layers on a substrate with corresponding intensity distribution in reciprocal space for lamellae lying (A) parallel to (B) perpendicular to or (C) at a given angle, γ, to a substrate. For (B) and (C) the intensity is distributed on rings in reciprocal space due to random arrangement of small grains in the plane of the film. The diagrams shown correspond to an angle of incidence $\alpha = 90°$. The scattering pattern seen in the SAXS experiment is constructed by taking the intersection of the scattering intensity in reciprocal space with the Ewald sphere, which for the case shown here ($\alpha = 90°$) corresponds to the k_x-k_z plane. The resulting pattern depends on the angle of incidence, α, as described in the text.

appears in the scattering pattern. If the lamellae are inclined at an angle $\gamma < 90°$ to the surface normal, four spots are observed for all $\alpha > (90° - \gamma)$ (Figure 1C). These four spots merge into a pair of equatorial reflections for $\alpha = 90° - \gamma$. For a given angle of incidence α, only lamellae with inclination $\gamma \geq (90° - \alpha)$ are observable.

The PS-*b*-PI under investigation showed a peak in the scattering intensity at $q = 0.197$ nm^{-1}, corresponding to a period of $L = 31.9$ nm. All time-resolved in-situ experiments were performed at an angle of incidence $\alpha = 45°$. Thus, only scattering arising from lamellae with $\gamma \geq 45°$ is observed. The azimuthal angular dependence of the scattering, integrated over the full width of the reflection in q, is shown in Figure 2 as a function of time for a sample under an 18 V/μm applied field. Four distinct patterns, characterizing different stages of the orientation process, were observed. Typical for the initial state is a weak, sometimes anisotropic, scattering pattern (curve A), indicating that the sample preparation process has oriented the lamellae mostly parallel to the substrate surface. After 30 s under the applied field the scattering pattern has substantially changed, and the intensity is concentrated around the equator ($\Omega = 90°$ and 270°, curve B). This arises from lamellae satisfying the specific condition that $\gamma \approx \alpha = 45°$ leading, initially, to the equatorial maxima at $\Omega = 90°$ and 270°. The overall intensity has increased, which means that stacks of the lamellae, previously unobservable ($\gamma <$ 45°), have begun to rotate into the direction of the applied field, i.e., toward $\gamma = 90°$. With increasing time, the maxima disappear and a more isotropic ring of

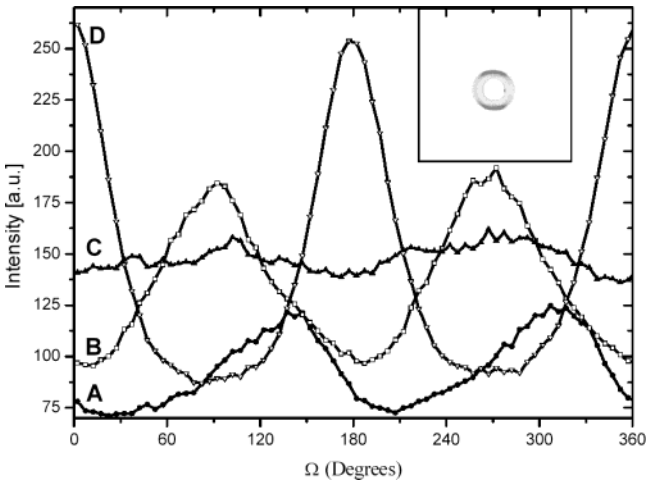

Figure 2. Series of SAXS measurements following the azimuthal angular dependence of the scattering pattern, integrated over the full width of the Bragg reflection, for electric field induced reorientation of a lamellar PS-*b*-PI diblock performed in situ. (A) Initial state, no field; (B) 18 V/μm, 30 s; (C) 18 V/μm, 60 s; (D) 18 V/μm, 240 s. The time indicated corresponds to the time since the electric field was switched on. The sequence of patterns is caused by a rotation of microdomains from an orientation close to parallel to the substrate to an orientation perpendicular to the substrate. The 2-D SAXS pattern corresponding to (D) is shown in the inset.

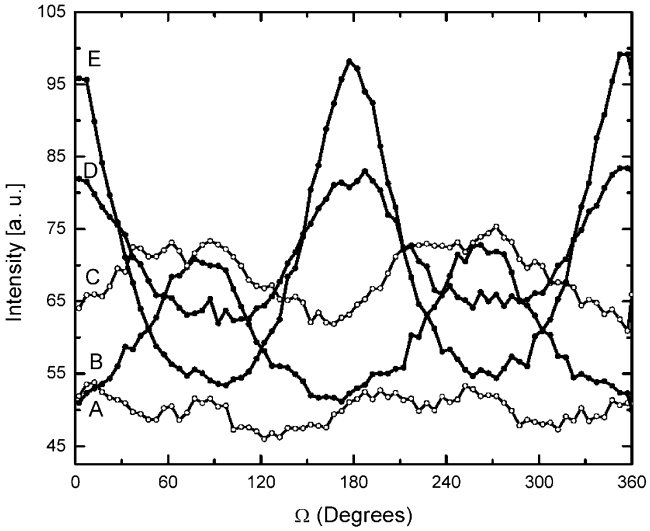

Figure 3. Series of SAXS measurements following the azimuthal angular dependence of the scattering of a SIS lamellar triblock material during alignment at 10 V/μm in situ. (A) 0 V/μm; (B) 10 V/μm, 15 min; (C) 10 V/μm, 30 min; (D) 10 V/μm, 45 min; (E) 15 V/μm, 30 min. The time indicated corresponds to the time since the electric field was switched on. The sequence of patterns observed is similar as in the case of the diblock copolymer system. A subsequent increase in field strength to 15 V/μm leads to improved alignment.

scattering is seen (curve C). This arises from many small grains of lamellar microdomains with orientations angles $\gamma \geq 45°$. Consequently, the applied field has removed the orientation initially present in the sample. With further annealing, strong meridional maxima are seen (curve D) from lamellae oriented perpendicular to the substrate ($\gamma = 90°$), i.e., parallel to the applied field.

In Figure 3, we show the results of the process of alignment for a SIS triblock copolymer under similar conditions. We observe the same sequence of scattering patterns as in Figure 2. Additionally, we show explicitly that upon application of a higher field the meridional

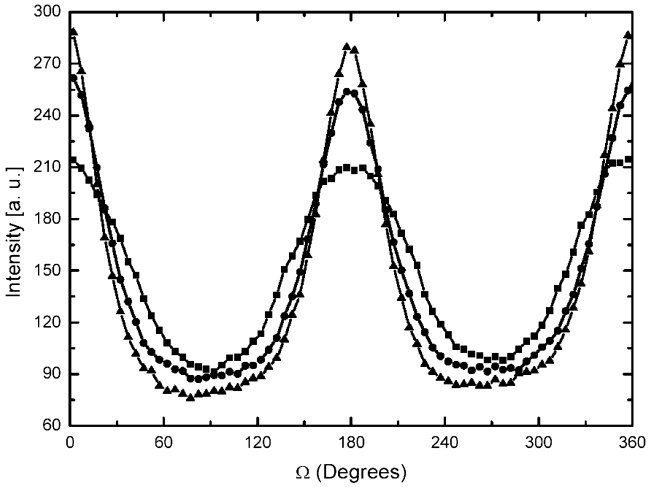

Figure 4. Azimuthal angle dependence of the scattering for a lamellar PS-*b*-PI after repeated application of the electric field while maintaining the temperature above T_g of the blocks. Without field the orientational distribution relaxes, repeated application of an electric field leads to an improved alignment. (●) 18 V/μm, 4 min; (■) 0 V/μm, 20 min; (▲) 18 V/μm, 15 min. The time indicated corresponds to the time since the electric field was switched on/off.

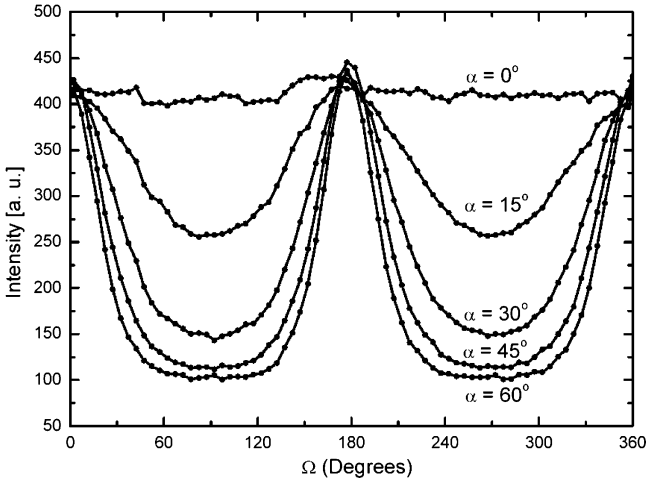

Figure 5. Azimuthal angular dependence of the Bragg reflection in the resulting final aligned state of lamellar PS-*b*-PI measured at different angles of incidence α. The patterns are caused by a multitude of small grains consisting of lamellar stacks aligned perpendicular to the substrate due to the electric field with a random orientation within the plane of the substrate.

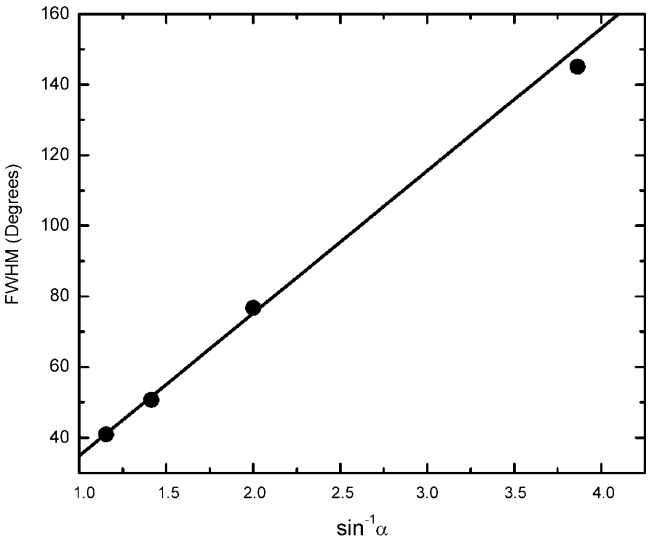

Figure 6. Fwhm of the peaks of the data shown in Figure 5 vs 1/sin α with α being the angle of incidence. Linear extrapolation to 1/sin α = 1; i.e., α = 90° gives a fwhm of the orientational distribution of the lamellae of $\Delta\Omega = 35°$, corresponding to an orientation parameter $S = -0.41$.

reflections intensify and sharpen (curve E). It should be noted that orientation occurs over a longer period of time with this triblock copolymer due primarily to its higher viscosity at $T = 130$ °C, the temperature at which the data were collected. There are two points to note about the similarity in the sequence of patterns observed. First, for the triblock copolymer, the experiment was performed at a temperature relatively close to the ODT, i.e., in a less strongly segregated state, whereas the diblock copolymer alignment was performed well below ODT, i.e., in the strongly segregated regime. Second, rheological studies have shown that diblock and triblock copolymers orient in distinctly different ways in shear flows.[32,33] However, this does not seem to be the case for the response to an applied electric field.

Let us now come back to a more detailed discussion of the data obtained from the diblock copolymer. After an initial alignment of the PS-*b*-PI for 4 min at 18 V/μm, the applied field was removed while keeping the system at 170 °C. Upon removal of the applied field, as shown in Figure 4, the peak intensity decreased within minutes and the full width at half-maximum intensity (fwhm) increased. However, the overall orientation of the microdomains was maintained. The sample was subsequently placed under an electric field of 18 V/μm for an additional 15 min. The orientation of the microdomains was seen to increase, as evidenced by the decrease in the fwhm. Thus, by allowing the system to relax between consecutive applications of a field, the alignment was enhanced. This suggests that the cycling of the electric field has allowed the copolymer to circumvent a kinetically trapped state to achieve a higher degree of alignment of the microdomains.

Figure 5 shows azimuthal scans of the diblock copolymer in the final aligned state for discrete values of α between 0° and 60°. The results are consistent with a film comprised of grains of lamellar microdomains oriented normal to the surface, where the grains are randomly oriented in the plane of the film. At α = 0°, an isotropic ring of scattering is observed, and as the sample is tilted to larger α, the alignment of the microdomains normal to the surface is evidenced by the appearance of two meridional reflections that get sharper at higher α. In Figure 6, the measured fwhm of the reflections is plotted as a function of 1/sin α, which allows for a linear extrapolation to α = 90° (i.e., 1/sin α = 1). The extrapolated fwhm is $\Delta\Omega = 35°$. This value corresponds to the fwhm of the orientation distribution in γ, describing the orientation of the lamellae. The meaning of this value becomes clearer by calculating a corresponding orientation parameter, S, based on the assumption that the underlying orientation distribution $g(\cos\gamma)$ is a Gaussian with its center at $\pi/2$ and with the experimentally determined fwhm ($\Delta\Omega = 35°$)

$$S \equiv \frac{3\langle\cos^2\gamma\rangle - 1}{2}$$

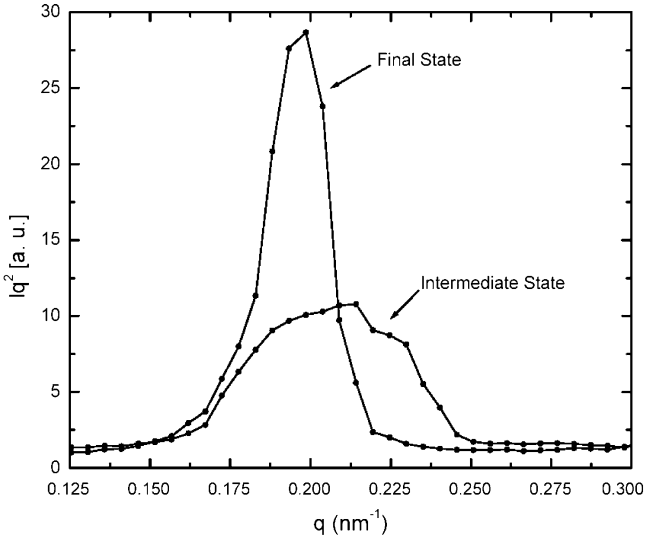

Figure 7. q dependence of the scattering intensity for the intermediate and final state of orientation of PS-*b*-PI during the electric field alignment process. Data taken at $\alpha = 45°$ correspond to the experiment shown in parts B and D of Figure 2 after applying field for 30 and 240 s, respectively. The broadening of the peak and the shift in q observed for the intermediate state indicates partial disordering of the microphase structure.

with

$$\langle \cos^2 \gamma \rangle = \frac{\int_0^\pi g(\cos \gamma) \cos^2 \gamma \sin \gamma \, d\gamma}{\int_0^\pi g(\cos \gamma) \sin \gamma \, d\gamma}$$

Perfect alignment would result in an $S = -0.5$. For our data, we calculate an orientation parameter S of -0.41. Note that this high degree of orientation was obtained within minutes. With extended annealing, even better orientation can be achieved.

The q dependence of the scattering observed for the intermediate stage during alignment of the copolymer reveals important insight into the orientation mechanism. Shown in Figure 7 is the q dependence of the scattering for PS-*b*-PI with $\alpha = 45°$ under 18 V/μm after 30 and 240 s, i.e., at an intermediate and final state of orientation, respectively. The initial peak position and that after full alignment are the same, corresponding to the equilibrium period of the lamellar microdomains. However, during orientation, the maximum of the peak moved to higher q (from 0.198 to 0.216 nm^{-1}), and the peak became asymmetric in shape. The asymmetric shape of the peak suggests the existence of a second peak located at higher q. This may arise from lamellae being deformed during orientation or a deformation-induced disordering of the copolymer.

Discussion

The data shown suggest a scenario by which the electric field induces a reorientation of an ordered copolymer. It is noteworthy that reorientation, under the conditions of this experiment, occurs at all, as most previous experiments were performed on copolymers close to the order−disorder transition temperature, quenched after spin-coating or in the presence of a solvent to enhance mobility. Here, the copolymer is well ordered initially, and a fast reorientation of the microdomains is seen to occur. In contrast to previous experiments,[20,25] an in-situ observation of an electric field induced intermediate state was selectively captured (trace B in Figure 2) during the realignment process of the copolymer melt. After alignment, the morphology consists of small grains of lamellar microdomains where the interfaces are aligned with the field but with a random orientation of the lamellar normals in the plane of the film. This result is not unexpected from symmetry considerations alone as there is a ring of preferred orientations, and without a special direction orthogonal to the electric field, one expects a distribution of these orientations after field alignment. Regardless whether alignment occurs via rotation of spherical domains or amplification of undulations in the orientation direction, the fundamental orienting unit has to be small. How the original morphology was transformed into a multitude of small grains undergoing alignment could not be observed directly in the scattering geometry chosen for this experiment (only lamellae with $\gamma \geq 45°$ are observable). A mechanism likely to occur was introduced by Onuki et al.,[34] namely an undulation instability leading eventually to a disruption of lamellae misaligned with respect to the electric field. Krausch and co-workers[20,21] showed that further orientation in solutions can occur via a rotation process during which intermediate orientations are visible. However, Figure 7 shows that the microphase structure in such an intermediate state is strongly perturbed. A substantial part of the sample shows a decrease in the spacing of the microdomains, and the correlation length is substantially reduced. The full width at half-maximum of the peak shown in Figure 7, $\Delta q \approx 0.058$ nm^{-1}, corresponds to a correlation length $\xi = 2\pi/\Delta q \approx 109$ nm, i.e., corresponding to only about 3 lamellar periods. These signatures are similar to the changes observed in the scattering function upon disordering at high temperatures, and we interpret them accordingly. As a consequence of the reduced order in the intermediate state, the structure obtained initially after realignment contains a large number of defects. This is consistent with the rapid reorganization taking place after cessation of the field along with a loss of orientation, as shown in Figure 4. The resulting higher degree of orientation obtained after renewed application of the electric field could then be explained by an increased domain size after reorganization, since the torque acting on a grain of lamellae is proportional to its volume.

The field strengths chosen for these experiments were observed to be necessary for realignment to occur. Lower field strengths resulted in no reorientation of the PS-*b*-PI domains over the time scale of our experiments. In comparison to PS-*b*-PMMA, therefore, the field necessary to orient the microdomains of PS-*b*-PI was ∼5−10 times higher. The driving force for alignment is proportional to the square of the product of the electric field and $\Delta\epsilon$, the difference in dielectric constants of the microdomains. Using tabulated values for the dielectric constants ($\epsilon_{PS} = 2.5$, $\epsilon_{PMMA} = 3.6$, $\epsilon_{PI} = 2.37-2.45$) at constant energy difference between parallel and perpendicular orientation, $E^{SI} \sim 10-30E^{SM}$. Since the dielectric constants of polymers are known to vary with temperature, dielectric measurements were performed as a function of temperature for all three materials. At 170 °C and 10 Hz, the dielectric constants were measured as $\epsilon_{PS} = 3.0$, $\epsilon_{PMMA} = 5.25$, and $\epsilon_{PI} = 2.81$. Using these values, $E^{SI} \cong 12E^{SM}$. Both results are consistent with the experimental observations.

Conclusions

The electric field induced orientation of an ordered, symmetric PS-*b*-PI diblock and SIS triblock copolymer melt was investigated by means of time-resolved small-angle X-ray scattering using a scattering geometry suitable for the study of thin film samples equipped with electrodes that are transparent to X-rays. The scattering patterns show contributions corresponding to a state of intermediate alignment with distinctly different peak shapes. This indicates partial disordering of the copolymer during reorientation. We relate this finding to the significant disruption that the original copolymer grains must undergo, so as to reduce their size such that a domain rotation can occur. The question as to which parameters determine the size of the rotating grains is not known at this point.

Acknowledgment. We are grateful to S. Bennett for technical support during the experiments at the NSLS. The authors thank the Department of Energy, Office of Basic Energy Science, and the National Science Foundation through the Materials Research Science and Engineering Center for support of this research. T.T.-A. acknowledges the support of the Deutsche Forschungsgemeinschaft.

References and Notes

(1) Bates, F. S.; Fredrickson, G. H. *Annu. Rev. Phys. Chem.* **1990**, *41*, 525.
(2) Hamley, I. W. *The Physics of Block Copolymers*; Oxford University Press: Oxford, 1998.
(3) Lodge, T. P. *Macromol. Chem. Phys.* **2003**, *204*, 265.
(4) Amundson, K.; Helfand, E.; Davis, D. D.; Quan, X.; Patel, S. S.; Smith, S. D. *Macromolecules* **1991**, *24*, 6546.
(5) Amundson, K.; Helfand, E.; Quan, X.; Smith, S. D. *Macromolecules* **1993**, *26*, 2698.
(6) Amundson, K.; Helfand, E.; Quan, X.; Hudson, S. D.; Smith, S. D. *Macromolecules* **1994**, *27*, 6559.
(7) Morkved, T. L.; Lu, M.; Urbas, A. M.; Ehrichs, E. E.; Jaeger, H. M.; Mansky, P.; Russell, T. P. *Science* **1996**, *273*, 93.
(8) Mansky, P.; DeRouchey, J.; Russell, T. P.; Mays, J.; Pitsikalis, M.; Morkved, T.; Jaeger, H. *Macromolecules* **1998**, *31*, 4399.
(9) Thurn-Albrecht, T.; DeRouchey, J.; Russell, T. P.; Jaeger, H. M. *Macromolecules* **2000**, *33*, 3250.
(10) Mansky, P.; Liu, Y.; Huang, E.; Russell, T. P.; Hawker, C. *Science* **1997**, *275*, 1458.
(11) Russell, T. P.; Thurn-Albrecht, T.; Tuominen, M.; Huang, E.; Hawker, C. J. *Macromol. Symp.* **2000**, *159*, 77.
(12) Kim, G.; Libera, M. *Macromolecules* **1998**, *31*, 2569.
(13) Kimura, M.; Misner, M.; Kim, S. H.; Xu, T.; Russell, T. P. *Langmuir* **2003**, *19*, 9910.
(14) Thurn-Albrecht, T.; Schotter, J.; Kastle, G. A.; Emley, N.; Shibauchi, T.; Krusin-Elbaum, L.; Guarini, K.; Black, C. T.; Tuominen, M. T.; Russell, T. P. *Science* **2000**, *290*, 2126.
(15) Black, C. T.; Guarini, K. W.; Milkove, K. R.; Baker, S. M.; Russell, T. P.; Tuominen, M. T. *Appl. Phys. Lett.* **2001**, *79*, 409.
(16) Montero, M. I.; Liu, K.; Stoll, O. M.; Hoffmann, A.; Akermann, J. J.; Martin, J. I.; Vicent, J. L.; Baker, S. M.; Russell, T. P.; Leighton, C.; Nogues, J.; Schuller, I. K. *J. Phys. D: Appl. Phys.* **2002**, *35*, 2398.
(17) Kim, D. H.; Lin, Z. Q.; Kim, H. C.; Jeong, U.; Russell, T. P. *Adv. Mater.* **2003**, *15*, 811.
(18) Park, M.; Harrison, C.; Chaikin, P. M.; Register, R. A.; Adamson, D. H. *Science* **1997**, *276*, 1401.
(19) Thurn-Albrecht, T.; Steiner, R.; DeRouchey, J.; Stafford, C. M.; Huang, E.; Bal, M.; Tuominen, M.; Hawker, C. J.; Russell, T. P. *Adv. Mater.* **2000**, *12*, 787.
(20) Böker, A.; Elbs, H.; Hansel, H.; Knoll, A.; Ludwigs, S.; Zettl, H.; Urban, V.; Abetz, V.; Muller, A. H. E.; Krausch, G. *Phys. Rev. Lett.* **2002**, *89*, 135502.
(21) Böker, A.; Knoll, A.; Elbs, H.; Abetz, V.; Muller, A. H. E.; Krausch, G. *Macromolecules* **2002**, *35*, 1319.
(22) Tsori, Y.; Andelman, D. *Macromolecules* **2002**, *35*, 5161.
(23) Kyrylyuk, A. V.; Zvelindovsky, A. V.; Sevink, G. J. A.; Fraaije, J. G. E. M. *Macromolecules* **2002**, *35*, 1473.
(24) Zvelindovsky, A. V.; Sevink, G. J. A. *Phys. Rev. Lett.* **2003**, *90*, 49601.
(25) Thurn-Albrecht, T.; DeRouchey, J.; Russell, T. P.; Kolb, R. *Macromolecules* **2002**, *35*, 8106.
(26) Landau, L. D.; Lifshitz, E. M. *Electrodynamics of Continuous Media*, 2nd ed.; Pergamon Press: New York, 1984; Vol. 8.
(27) Hsieh, H. L.; Quirk, R. P. *Anionic Polymerization: Principles and Practical Applications*; Marcel Dekker: New York, 1996.
(28) Fredrickson, G. H.; Helfand, E. *J. Chem. Phys.* **1987**, *87*, 697.
(29) Buzza, D. M. A.; Fzea, A. H.; Allgaier, J. B.; Young, R. N.; Hawkins, R. J.; Hamley, I. W.; McLeish, T. C. B.; Lodge, T. P. *Macromolecules* **2000**, *33*, 8399.
(30) Buzza, D. M. A.; Hamley, I. W.; Fzea, A. H.; Moniruzzaman, M.; Allgaier, J. B.; Young, R. N.; Olmsted, P. D.; McLeish, T. C. B. *Macromolecules* **1999**, *32*, 7483.
(31) Johnson, J. M.; Allgaier, J. B.; Wright, S. J.; Young, R. N.; Buzza, N.; McLeish, T. C. B. *J. Chem. Soc., Faraday Trans.* **1995**, *91*, 2403.
(32) Tepe, T.; Hajduk, D. A.; Hillmyer, M. A.; Weimann, P. A.; Tirrell, M.; Bates, F. S.; Almdal, K.; Mortensen, K. *J. Rheol.* **1997**, *41*, 1147.
(33) Riise, B. L.; Fredrickson, G. H.; Larson, R. G.; Pearson, D. S. *Macromolecules* **1995**, *28*, 7653.
(34) Onuki, A.; Fukuda, J. *Macromolecules* **1995**, *28*, 8788.

MA034739F